International Journal of Future Generation Communication and Networking
Vol. 13, No. 1, (2020), pp. 985-998

# Wireless Capsule Endoscopy Image Classification Model to Detect Gastro Intestinal Tract Diseases Using Visual Words Based on Feature Fusion

R. Ponnusamy, Department of Computer and Information Science, Annamalai University, Chidambaram, India. Email:povi2006@gmail.com
S. Sathiamoorthy, Tamil Virtual Academy, Chennai, India. Email: ks_sathia@yahoo.com

## Abstract

*This work emphasis on Gastrointestinal (GI) disease diagnosis using Wireless Capsule Endoscopy (WCE) images. The recent researches in medical field are widely based on severe health illness such as cancer, diabetes, Alzheimer, Parkinson and heart diseases. These researches mainly focus on finding a new diagnosing method after the occurrence of the diseases. Consequently, there is a need to determine a new methodology for early stage diagnosing of diseases. Most diseases such as bleeding, ulcer and tumour in the GI tract can be cured or controlled in their early stages, otherwise it will deteriorate into cancer or some other vital diseases. In this work, the detection of pylorus, polyps, Z-line, cecum, ulcer and esophagitis are carried out by using WCE images. Although, these abnormalities are not harmful, it is pivotal to diagnose in the initial stage in order to avoid the development of severity in future. The WCE provides a number of images per second and hence it is difficult to identify the type of disease from the numerous identical images. Therefore, the classification of GI Tract Diseases from the images requires a new technique for accurate diagnosis. In this paper, features are extracted by Centre Symmetric-Local Binary Pattern (LBP), Auto Color Correlogram and Speeded Up Robust Feature (SURF) and it is further followed by K means clustering, Support Vector Machine (SVM) and Particle Swarm Optimization- Support Vector Machine (PSO-SVM) classification. The efficiency of these techniques is analysed by means of performance. The results obtained shows that the proposed method of PSO-SVM with the combined CS-LBP+ACC+SURF gives better classification results and well suited for particular set of images. In future, a greater number of images have to be processed for accurate analysis as well as to try with some other classifiers.*

***Keywords:*** *WCE, SURF, CS-LBP, ACC, K-means, SVM, PSO-SVM GI tract diseases,*

## Introduction

The WCE is essential for viewing the GI tract noninvasively in order to identify the affected parts in stomach, esophagus, small intestine, large intestine, rectum, liver, pancreas and gallbladder [1]. A capsule endoscopy camera is present inside the capsule and it is swallowed by the patient [2]. It could take a greater number of GI tract pictures and transmit it into a recording device which is tied around the patient waist. These recorded images are helpful to analyse various GI diseases. In this work, pylorus, polyps, Z-line, cecum, ulcer and esophagitis are considered as it can be evaded if these abnormalities are treated earlier. Firstly, Polyps are abnormal growth of tissue in the colon or rectum and it is appeared as flat or like stalk [3]. There are different types of polyps in which some are benign and some are malignant. It is therefore vital to detect the non-benign in advance. Similarly, ulcer is also a life-threatening disease if it is not treated properly. It is caused by bacterial infection called Helicobacter pylori.


ISSN: 2233-7857 IJFGCN

Stomach and duodenal ulcers are the most common type in which stomach ulcer can cause complications such as major bleeding and perforation. Therefore, it is prominent to treat and diagnose prior to its development. On the other hand, pylorus is a valve that connects stomach to the duodenum. The function of pylorus is to prevent the intestinal items from entering the stomach when the contraction of small intestine takes place and also to control the passage of indigested food particles into the intestine. Pyloric Stenosis affects the newborn and infants and can cause dehydration and electrolyte imbalance. It requires surgical treatment to recover and hence it is crucial to view the pylorus region. Furthermore, Z line is a region that connects the esophagus to the stomach and the assessment of this z line could help to determine the presence of diseases as well as to describe the pathology in the esophagus. Esophagitis is an inflammation of the esophagus and can cause chest pain, difficulty in swallowing and acid regurgitation. Hence esophagitis has to be diagnosed in the initial stage otherwise it will cause damage to the lining of the esophagus and affect its normal function. Lastly, the cecum is located at the beginning of the large intestine. It plays a significant role in the formation of feces. The prevalence of cecal diverticulitis disease results in abdominal pain and other symptoms. Therefore, cecum is also a fundamental part to consider for early identification of disease.

## Related Work

Amit kumar et al presented a method to detect bleeding and non-bleeding regions which involves normalization of RGB (red green blue) colour plane, proposed region of interest (ROI) and proposed feature extraction and it was further followed by K-nearest neighbour classification [4]. As per the proposed technique, morphological erosion and dilation was carried out to detect the bleeding region. After the bleeding image detection, video analysis was done to remove falsely detected image. In addition, the proposed technique was compared with other methods and performance metrics shows nearly 97%accuracy was achieved by the proposed method. Ouiem Bchir et al, proposed multiple bleeding detection in WCE [5]. In this paper, visual properties were captured from different visual descriptors in each WCE frame to obtain numerous bleeding spots. They suggested Hue, Saturation, Value (HSV) colour moment descriptors were better than local colour moments, RGB colour histogram, LBP, DWT and Gabor. They also compared the performance of the proposed technique with KNN (k Nearest Neighbourhood) and SVM classifier. The results show that 90%accuracy was obtained from the proposed method. Mohsen et al, presented a method for automatic detection of bleeding region [6]. The method involves colour channels selection and Multilayer Perceptron (MLP) classification. This neural network is then quantized and tested by simulation using WCE bleeding images. They also compared MLP with SVM classifier and inferred that the proposed technique provides better accuracy. Similarly, Meryem et al, introduced an ulcer detection system in which multi scale LBP was performed to the input RGB image and followed by Laplacian pyramid transform [7]. This method was then compared with curvelet based LBP. The experimental results however show that 95% accuracy for the proposed method. Dassopoulos et al, presented a novel method for detecting adenomatous polyps using WCE images [8]. In this work, they utilized colour layout descriptor, edge histogram descriptor, colour and edge directive descriptor, fuzzy colour and texture histogram descriptor, Gabor filter


ISSN: 2233-7857 IJFGCN

descriptor, grey level co-occurrence matrices, tamuras texture features, edge frequency descriptors, autocorrelation feature and primitive length feature. These features were calculated over the ROI using white light (WL)input image and narrow band imaging (NBI) input image. They grouped 3 feature sets using WL, NBI and both type input images. Furthermore, classification by Random Forest classifier in Waikato Environment for Knowledge Analysis (WEKA) toolbox was carried out and used WEKA software library for attribute selection. They inferred that colour and edge directivity; fuzzy colour and texture histogram descriptors were better than the rest. Jia et al, proposed a patent work (United States) related to polyp detection using pruning technique in WCE images [9]. In this paper, regression is performed in the extracted features to check whether the identified polyp is the actual polyp or not. They are then calculated image gradients for each ROI in polyp images. After gradient alignment and accumulation of magnitude histogram, histogram variation is calculated between smallest and largest ROI in polyp image. In another work by Said Charfi et al, Local Fractal Dimension (LFD) feature extraction in the key points detected by Scale Invariant Feature Transform (SIFT)was carried initially [10]. Later, texture features were derived by using Uniform Local Binary Pattern (LBPu) and Complete LBP(CLBP). Then classification was done by SVM, MLP and Random Forest classifiers. This proposed method was compared with state of art methods and concluded that the accuracy obtained by the combination of SIFT, LFD and LBPu provides better performance and it was 97.98%. Mustain et al, suggested a method for polyp identification by means of wavelet colour texture feature extraction and Convolutional Neural Network (CNN) feature extraction [11]. Then the features extracted were classified by SVM. The experimental results show that this method outperforms the state of art methods and the accuracy obtained by this method was 98.34%. Yixuan Yuan et al, presented a novel technique called discriminative joint feature topic model (DJTM) with dual constraints for WCE classification [12]. The abnormalities considered were bleeding, polyp and ulcer. In DJTM, colour and texture features were extracted and clustered by K means to generate Bag of Words (BOW) histograms. Secondly, visual word importance was calculated and local image manifold was modelled by a nearest neighbour graph. Finally, visual word importance and local image manifold were incorporated to Probabilistic Latent Semantic Analysis (PLSA). Then the obtained features were given to SVM classifier. Confusion matrix was created to check the performance of the proposed method and it shows 97% overall accuracy. Similarly, Yixuan Yuan et al, introduced Saliency and Adaptive Locality constrained Linear Coding (SALLC) method to detect polyp, ulcer and bleeding using WCE videos [13]. The colour scale invariant feature transform was used to extract colour texture features and k-means clustering was applied on these features to acquire visual words. It was then processed by SALLC algorithm and further followed by max pooling method for image representation. SVM classifier classified these abnormalities and the overall accuracy achieved was 88.61%.

**Proposed Method**

In this work, three feature extraction methods such as CS-LBP, ACC and SURF are combined to obtain all the useful features in an image. These features are combined as CS-LBP+SURF, ACC+SURF and CS-LBP+ACC+SURF. The extracted features by CS-LBP, ACC and SURF

are grouped into clusters by means of K- means clustering which is further followed by SVM and PSO-SVM classification. In this work, the assumed codebooks are 50, 100, 150 and 200

and the results show better accuracy when the number of codebooks is 100. In other considered codebooks, the problem in grouping ended up in false detection. It means the clustering method groups the background features rather than the region of interest and hence reduce the accuracy level. The proposed work is shown in Fig.1

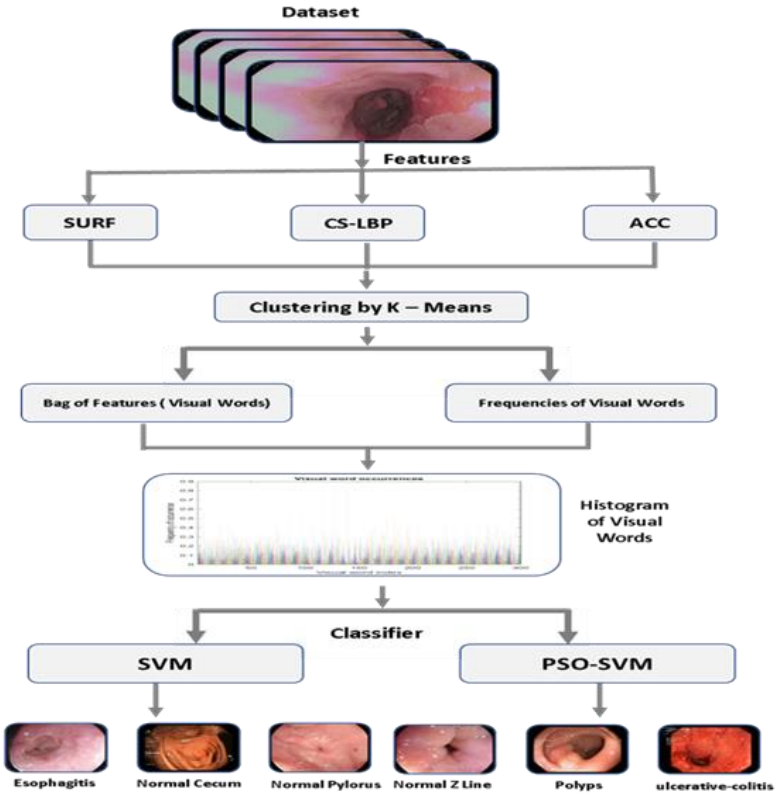


Figure 1: Proposed work

**SURF:**

The WCE takes numerous images in the GI tract and thus it is a challenge to differentiate the region of interest. Hence, SURF feature is considered in this paper in order to identify the required feature from the huge WCE images. The SURF algorithm consists of two main steps which are feature detection and feature description. The SURF feature detection depends on scale-space representation, combined with first and second order differential operators. These operations are speeded up by the use of box filter techniques. Thus, Box space is used to differentiate from Gaussian scale-space. The Gaussian scale space is obtained by convolution of initial images with Gaussian kernels. The SURF feature detection is based on Hessian matrix since it possesses better performance and accuracy [14]. In image I, x = (x, y) is the given point, the Hessian matrix H (x, σ) in x at scale σ, can be defined as

$$H(x, \sigma) = \boldsymbol{Lxx}\ (\boldsymbol{x}, \boldsymbol{\sigma})\ \boldsymbol{Lxy}\ (\boldsymbol{x}, \boldsymbol{\sigma})$$

$$\boldsymbol{Lyx}(\boldsymbol{x},\boldsymbol{\sigma}) \quad \boldsymbol{Lyy}(\boldsymbol{x},\boldsymbol{\sigma})$$

Where Lxx (x, σ) is the convolution result of the second order derivative of Gaussian filter $\partial 2 / \partial x 2[\ g(\sigma)]$ with the image I in point x, and similarly for Lxy (x, σ) and Lyy (x, σ).
The ultimate aim in interest point detection is to find peculiar locations in WCE image such as corners, junctions etc. The selection of the interest point is performed along with the estimation of similarity transform parameters such as location, scale and orientation. Interest points are defined as local maxima and these maxima are detected by considering neighbourhood and performing a comparison of every vowel of the discrete box space with its 26 nearest neighbours. On the other hand, feature descriptor used in SURF is based on the sum of the Haar wavelet response around the point of interest, which makes it competent to be enumerated with the aid of internal image. SURF descriptors are used to locate and recognize objects, people, to reconstruct 3D images, to track objects and to extract points of interest.

**CS-LBP:**

CS-LBP describes the texture features present in an image and for each pixel in an image the CS-LBP pattern could be calculated by comparing its pixel value with the neighbourhood pixel values. The CS-LBP feature vector is created by the following algorithmic steps [15]. Firstly, the window considered is divided into cells and each pixel in a cell is compared to each of its eight neighbourhood. When the centre pixels value is greater than the neighbour's value, then write zero. Otherwise, write one and gives an eight-digit binary number. Furthermore, compute the histogram, over the cell, of the frequency of each number occurring. This histogram can be seen as a 256-dimensional feature vector. Finally, normalize the histogram and connect the normalized histogram of all cells. This provides the feature vector for the entire window. The CS-LBP operator uses the centre pixel value as threshold to the 3*3 neighbour pixels. Threshold operation will create a binary pattern denoting texture characteristic. The equation of CS-LBP is

$$\text{CS-LBP}\ (x_c, y_c) = \sum_{n=0}^{7} 2^n g\ (I_n - I(x_c - y_c))$$

CS-LBP $(x_c, y_c)$ is an CS-LBP value at the centre pixel $(x_c, y_c)$. $I_n$ and $I(x_c - y_c)$ are the values of neighbour pixel and centre pixel respectively. Index n is the index of neighbour pixels. The function g(x) will be 0 if x is less than 0 and g(x)=1 if x≥0.

**Auto Color Correlation**

The definition of the correlogram is the following [16][17][18]. Let [D] denote a set of D fixed distances {d1… dD}. Then the correlogram of the image I is defined for level pair (gi, gj) at a distance d .

$$\gamma_{g_i,g_j}^{(d)}(\mathbf{I}) \equiv \Pr_{p_1 \in \mathbf{I}_{g_i}, p_2 \in \mathbf{I}} \left[ p_2 \in \mathbf{I}_{g_j} \middle| |p_1 - p_2| = d \right]$$

Which gives the probability that given any pixel p1 of level gi, a pixel p2 at a distance d in certain direction from the given pixel p1 is of level gi. Autocorrelogram captures the spatial correlation of identical levels only:

$$\alpha_g^{(d)}(\mathbf{I}) = \gamma_{g,g}^{(d)}(\mathbf{I})$$

It gives the probability that pixels p1 and p2, d away from each other, are of the same level gi. The distance measure between the histograms, autocorrelograms, and correlograms is the L1-norm that is computationally light method and used in [16] and [17][19].

**BOW**

Bag of words is to portray an image as a set of features. Features involves key points which are the unique points in an image and also includes descriptors [20]. These are used to build the vocabularies and depict each image as a frequency histogram of features. The construction of bag of visual words comprises of feature detection, descriptors extraction from each input image and building a visual dictionary. These feature detection and descriptor extraction can be done by using SURF algorithm. In addition, clusters are formed from the descriptors by means of K means clustering. The centre of each cluster is used as the visual dictionary vocabularies. Finally, frequency histogram is created from the vocabularies for each image in order to represent the bag of visual words [21]. The process of K means clustering involved in BOW is described below.

**K -Means clustering:**

K means clustering identify unknown groups of data from complex data sets and it is also more suitable for large number of datasets. k means improves clustering accuracy and it does not take more time in classifying identical features [22]. The below flowchart describes the k means algorithm.

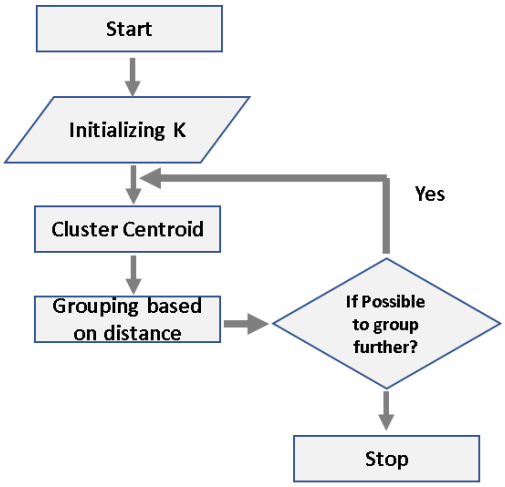


**Figure 2: K-means Algorithm**

**SVM:**

In WCE images the features are more and hence it is difficult to classify the diseases in GI tract. Therefore, SVM classifier is used in this work as it is more effective when the features are high. In SVM, there are four basic types of kernels which are linear, polynomial, Radial Basis Function (RBF) and sigmoid. In this work, RBF kernel function is utilized mainly


ISSN: 2233-7857 IJFGCN

because of their localized and finite responses across the entire range of the real x axis [23]. The RBF kernel (Wikipedia) is defined as

$$K(x, x^1) = \exp(-\| x-x^1\|^2/2\sigma^2)$$

Where x and $x^1$ are vectors of feature space, σ is a free parameter.

SVM is based on finding a hyperplane that best divides a dataset into two classes and support vectors are the data points nearest to the hyperplane. SVM creates a feature space that represents a finite dimensional vector space. In mathematical form, SVM create linear separating hyperplanes in high-dimensional vector spaces. Non-linear data can also be classified by customized hyperplanes. The most appropriate classification occurs when such hyperplanes gives maximal distance to the nearest training data points [24]. Training for SVM involves transforming input data to a high dimensional feature space and solving a quadratic optimization to suit an optimal hyperplane in order to classify the transformed features into two classes [25][26].

**PSO-SVM**

Particle swarm optimization is an evolutionary computation technique proposed by Kennedy and Eberhart. It is a population-based stochastic search process, modeled after the social behavior of a bird flock [27, 28]. It is similar in spirit to birds migrating in a flock toward some destination, where the intelligence and efficiency lie in the cooperation of an entire flock [29]. PSO algorithms make use of particles moving in an *n*-dimensional space to search for solutions for *n*-variable function optimization problem. All particles have fitness values which are evaluated by the fitness function to be optimized and have velocities which direct the flying of the particles. The particles fly through the problem space by following the particles with the best solutions so far. PSO is initialized with a group of random particles (solutions) and then searches for optima by updating each generation [30][31].

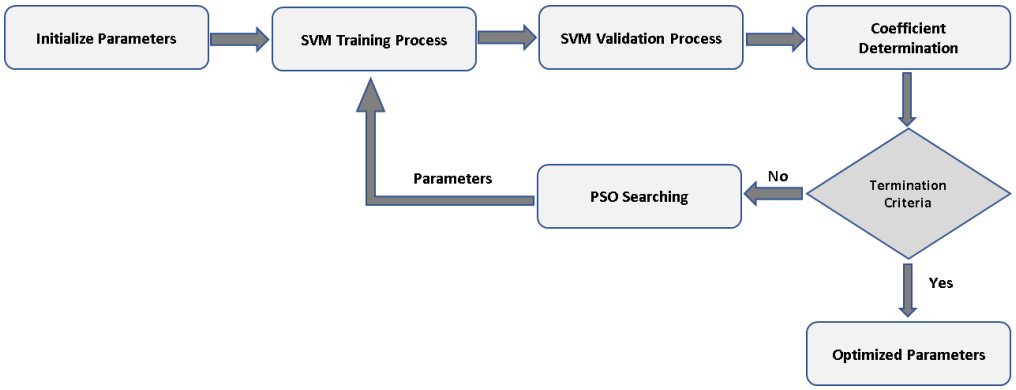


Figure.3 SVM-PSO algorithm

SVM also has a drawback that limits the use of SVM on academic and industrial platforms: there are free parameters (SVM hyperparameters and SVM kernel parameters) that need to be defined by the user. Since the quality of SVM regression models depends on a proper setting of these parameters, the main issue for practitioners trying to apply SVM is how to set these parameter values (to ensure good generalization performance) for a given training dataset.

SVM based on PSO optimizes two important hyperparameters $C$ and $\varepsilon$ using PSO. The hyperparameter $C$ determines the trade-off between the model complexity and the degree to which deviations larger than $\varepsilon$are tolerated. A poor choice of $C$ will lead to an imbalance between model complexity minimization (MCM) and empirical risk minimization (ERM). The hyperparameter $\varepsilon$ controls the width of the $\varepsilon$-insensitive zone, and its value affects the number of SVs used to construct the regression function. If $\varepsilon$ is set too large, the insensitive zone will have ample margin to include data points; this would result in too few SVs selected and lead to unacceptable "flat" regression estimates [32].

**Result & Discussion**

**[1] Data Collection**

The proposed method is analysed by using 900 WCE images which includes150 esophagitis images, 150 ulcer images, 150 polyp images, 150 z-line images, 150 cecum images and 150 pylorus images. These WCE images are selected from KVASIR dataset [3]. KVASIR is a dataset containing images from inside the gastrointestinal tract that are annotated and verified by experienced endoscopists. The images possess different resolution from 720*576 up to 1920*1072 pixels.

**[2] Performance Analysis**

The performance evaluation of the proposed method for GI tract abnormalities detection is calculated by means of sensitivity, specificity and accuracy [33]. The sensitivity is the ability of a test to identify correctly those with the disease. The specificity is the ability of a test to detect correctly those without the disease. The accuracy is the ability of a test to differentiate correctly the diseased and the non-diseased images. These indexes are calculated in terms of True Positive (TP), True Negative (TP), False Positive (FP) and False Negative (FN). TP is the number of correctly identified samples and TN is the number of correctly identified negative samples. FP is the number of wrongly identified samples and FN is the number of wrongly identified negative samples. These measures are defined as

- Sensitivity or Recall (REC) = TP/ (TP + FN)
- Specificity (SPEC) = TN/ (TN + FP)
- Accuracy (ACC) = (TP + TN)/ (TP+FP+FN+TN)

In our proposed work, the images are extracted by using CS-LBP, ACC and SURF. These features are combined as CS-LBP+SURF, ACC+SURF and CS-LPB+ACC+SURF. The images are clustered into four major sections for the analysis and the number of codebook size assumed are 50, 100, 150 and 200. The codebook size is calculated for CS-LBP+SURF, ACC+SURF and CS-LBP+ACC+SURF. The performance of varying codebook size for 6 classes using combined CS-LBP+ACC+SURF feature with SVM and PSO-SVM for these images and the results obtained are given below in Fig.3 and 4.

When then codebooks are hundred, pylorus is determined exactly as pylorus, Nonetheless, most of the other images are recognized as pylorus. In the same way, polyps, ulcer, cecum and esophagus are perceived correctly with minor errors.


ISSN: 2233-7857 IJFGCN

It is also found that when the number of clusters are high, the accuracy is also high. The datasets are also tested by considering the number of clusters as 150 and 200 and the result implies the same as like in 100 clusters. Therefore, assuming 100 clusters is chosen for accurate analysis of the considered diseases as shown in Fig.4 and 5.

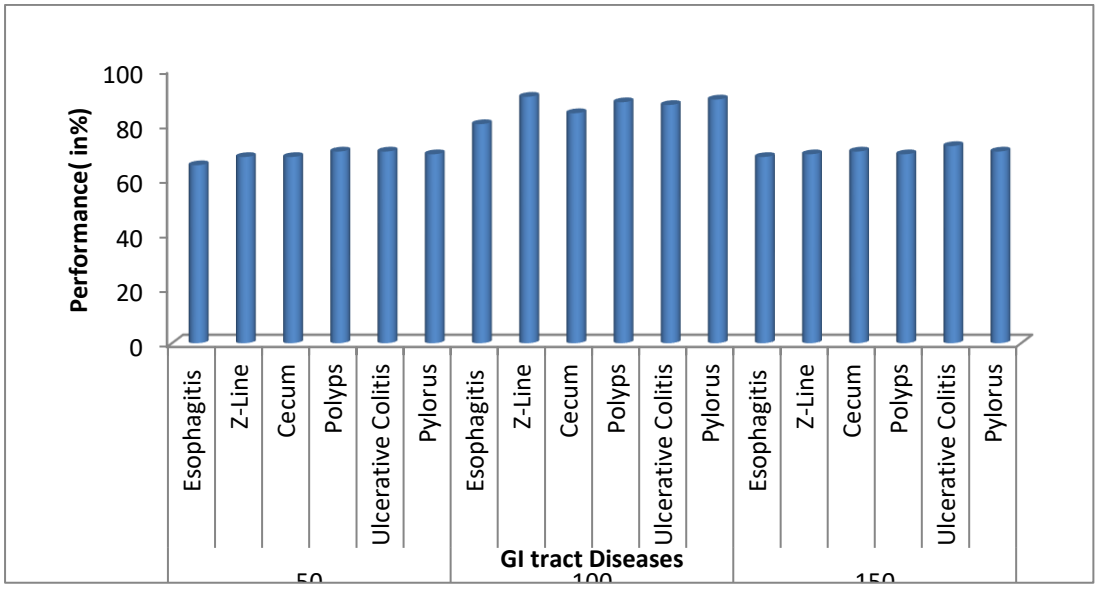


Figure.4 Performance of varying codebook size for 6 classes using CS-LBP+ACC+SURF features using SVM

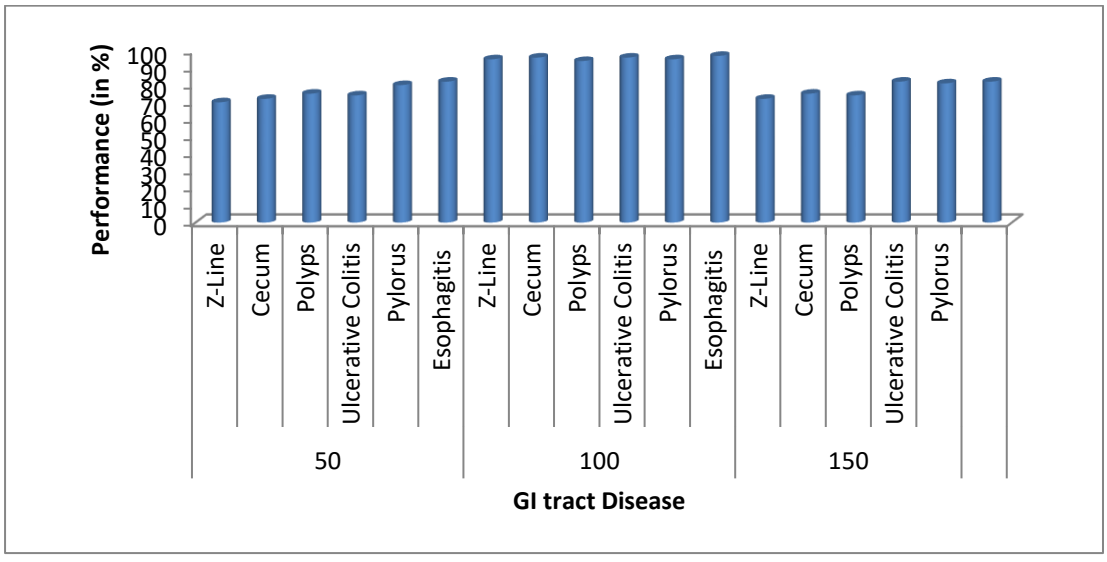


Figure.5 Performance of varying codebook size for 6 classes using CS-LBP+ACC+SURF features using PSO-SVM

The performance of various GI tract diseases using SVM with combined features such as CS-LBP+SURF, ACC+SURF and CS-LBP+ACC+SURF is shown in Table 1. From this Table 1. we analysis the performance of GI tract diseases while calculating the evaluation matrices such as Accuracy, sensitivity and Specificity. While comparing each class with combined features with proposed method PSO-SVM shows an accuracy of 80.02 % for Esophagitis, 90.08% for Z-

Line, 84.01% for cecum, 88.09% for Polyps, 87.0% for Ulcerative Colitis and 89.06% for Pylorus is obtained.

Table 1: Performance of GI tract diseases using SVM with CS-LBP+SURF, ACC+SURF and combined CS-LBP+ACC+SURF

| GI Tract Diseases | Performance ( in%) | CS-LBP+SURF | ACC+SURF | CS-LBP+ ACC+SURF |
|---|---|---|---|---|
| **Esophagitis** | **Accuracy** | **73.50** | **76.01** | 80.02 |
| | **Sensitivity** | **73.30** | **76.09** | **79.23** |
| | **Specificity** | **93.28** | **90.01** | **79.01** |
| **Z-Line** | **Accuracy** | **75.01** | **80.01** | **90.08** |
| | **Sensitivity** | **75.09** | **79.08** | **89.12** |
| | **Specificity** | **93.25** | **90.23** | **88.02** |
| **Cecum** | **Accuracy** | **80.02** | **82.23** | 84.01 |
| | **Sensitivity** | **79.01** | **80.01** | **83.01** |
| | **Specificity** | **93.6** | **90.03** | **80.02** |
| **Polyps** | **Accuracy** | **84.31** | **80.01** | **88.09** |
| | **Sensitivity** | **83.20** | **79.08** | **87.01** |
| | **Specificity** | **95.12** | **89.02** | **79.01** |
| **Ulcerative Colitis** | **Accuracy** | **82.20** | **85.01** | **87.0** |
| | **Sensitivity** | **82.01** | **84.08** | **87.02** |
| | **Specificity** | **93.25** | **89.21** | **84.01** |
| **Pylorus** | **Accuracy** | **88.01** | **88.21** | 89.06 |
| | **Sensitivity** | **88.02** | **88.05** | **89.57** |
| | **Specificity** | **92.25** | **90.01** | **88.02** |

The performance of various GI tract diseases using proposed PSO-SVM with combined features such as CS-LBP+SURF, ACC+SURF and CS-LBP+ACC+SURF is shown in Table 2. we analysis the performance of GI tract diseases is calculated by using evaluation matrices such as Accuracy, sensitivity and Specificity. While comparing each class with combined features with proposed method PSO-SVM shows an accuracy of 95.02 % for Esophagitis, 96.08% for Z-Line, 94.23% for cecum, 96.03% for Polyps, 95.23% for Ulcerative Colitis and 97.02% for Pylorus is obtained. From this Table 1&2, the proposed method of PSO-SVM shows better accuracy for 6 class of GI tract diseases than SVM.

Table 2: Performance of GI tract diseases using SVM_PSO with CS-LBP+SURF, ACC+SURF and combined CS-LBP+ACC+SURF

| GI Tract Diseases | Performance(in%) | CS-LBP+SURF | ACC+SURF | CS-LBP+ ACC+SURF |
|---|---|---|---|---|
| **Esophagitis** | **Accuracy** | **80.05** | **86.01** | **95.02** |
| | **Sensitivity** | **80.03** | **85.08** | **94.08** |



ISSN: 2233-7857 IJFGCN

| | | | | |
|---|---|---|---|---|
| | **Specificity** | **90.08** | **90.02** | **92.0** |
| **Z-Line** | **Accuracy** | **86.01** | **90.05** | **96.08** |
| | **Sensitivity** | **86.05** | **90.01** | **95.02** |
| | **Specificity** | **94.25** | **89.01** | **92.0** |
| **Cecum** | **Accuracy** | **88.01** | **90.01** | **94.23** |
| | **Sensitivity** | **87.95** | **90.08** | **93.01** |
| | **Specificity** | **93.6** | **90.01** | **90.9** |
| **Polyps** | **Accuracy** | **90.91** | **92.05** | **96.05** |
| | **Sensitivity** | **90.20** | **92.01** | **95.08** |
| | **Specificity** | **94.12** | **90.34** | **90.09** |
| **Ulcerative Colitis** | **Accuracy** | **85.20** | **88.01** | **95.23** |
| | **Sensitivity** | **84.71** | **87.05** | **95.02** |
| | **Specificity** | **92.25** | **90.02** | **90.64** |
| **Pylorus** | **Accuracy** | **90.01** | **95.05** | **97.02** |
| | **Sensitivity** | **90.20** | **94.08** | **96.08** |
| | **Specificity** | **96.25** | **93.01** | **93.34** |

Table 3. Confusion matrix for WCE image classification for SVM with combined CS-LBP+ACC+SURF

| | **Esophagitis** | **Z-Line** | **Cecum** | **Polyps** | **Ulcerative Colitis** | **Pylorus** | **Sensitivity** |
|---|---|---|---|---|---|---|---|
| **Esophagitis** | **80** | 8 | 2 | 7 | 3 | 0 | 80 |
| **Z-Line** | 10.05 | **90** | 0 | 8.23 | 10.05 | 6.06 | 90 |
| **Cecum** | 0 | 6 | **84** | 4 | 2 | 2 | 84 |
| **Polyps** | 0 | 0 | 8 | **88** | 4 | 0 | 88 |
| **Ulcerative Colitis** | 5 | 0 | 0 | 6 | **87** | 4 | 87 |
| **Pylorus** | 1 | 2 | 8 | 0 | 0 | **89** | 89 |
| **Specificity** | 79 | 88 | 80 | 79 | 84 | 88 | |

Table 4. Confusion matrix for WCE image classification for SVM_PSO with combined CS-LBP+ACC+SURF

| | **Esophagitis** | **Z-Line** | **Cecum** | **Polyps** | **Ulcerative Colitis** | **Pylorus** | **Sensitivity** |
|---|---|---|---|---|---|---|---|
| **Esophagitis** | **95** | 0 | 2 | 0 | 3 | 0 | 95 |



ISSN: 2233-7857 IJFGCN

| | | | | | | | |
|---|---|---|---|---|---|---|---|
| **Z-Line** | 0 | **96** | 0 | 2 | 0 | 2 | 96 |
| **Cecum** | 0 | 2 | **94** | 2 | 2 | 0 | 94 |
| **Polyps** | 0 | 0 | 4 | **96** | 0 | 2 | 96 |
| **Ulcerative Colitis** | 0 | 0 | 0 | 3 | **95** | 2 | 95 |
| **Pylorus** | 0 | 0 | 0 | 0 | 3 | **97** | 97 |
| **Specificity** | 92 | 92 | 90 | 92 | 90 | 93 | |

Table 3 and 4 shows confusion matrix for WCE images classification for SVM and PSO-SVM with combined CS-LBP+ACC+SURF. The proposed method PSO-SVM with CS-LBP+ACC+SURF provides better accuracy when compared with SVM. It is clear from the table 1 and 2, while combining the features CS-LBP, ACC and SURF the performance will increases. This could indicate that the proposed work is best suited even if the classes are high.

Performance of GI tract diseases classification using SVM and PSO-SVM with combined features CS-LBP+ACC+SURF as shown in Fig.6. The proposed method gives better accuracy when compared with other methods.

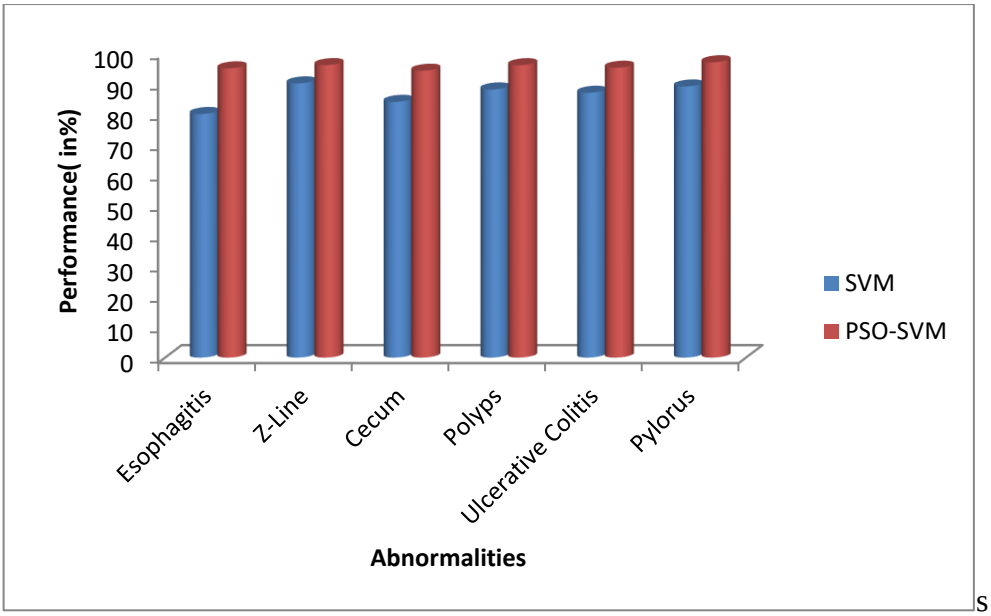


Figure 6. Performance of GI tract disease classification using SVM and PSO-SVM

## Conclusion

In this work, a novel method is introduced for early diagnosis of GI tract diseases using WCE images. It is a challenge to detect the GI tract diseases, since the obtained images from WCE possess common features. These identical features may result in false identification of diseases. For instance, in order to determine the presence of ulcer in WCE image, there is a possibility to distinguish it as polyps. Therefore, to avoid this problem the proposed combination of techniques such as SURF, ACC and CS-LBP along with PSO-SVM are best suited and hence it is suggested for detecting GI tract diseases. The efficiency of this method is calculated by

means of performance metrics which shows 96.66% when the number of clusters are increased to hundred. In future, it is imperative to test this method for accurate classification of various GI tract diseases using greater number of input images. Moreover, the PSO-SVM classifier used in this method has to be replaced by other classifiers for further analysis.

## References

[1] ASGE Technology Committee, "Technology status evaluation report", Gastrointestinal Endoscopy Journal, Vol.78, No.6,2013.
[2] Guobing pan, Litong Wang, "Swallowable Wireless Capsule Endoscopy: Progress and technical challenges", Gastroenterology Research & Practice, 2012.
[3] Konstantin Pogorelov, Kristin Ranheim Randel, Carsten Griwodz, Sigrun Losada Eskeland, Thomas de Lange, Dag Johansen, Concetto Spampinato,Duc-tien Dang- Nguyen, Concetto Spampinato,Mathias lux, Peter Thelin Schmidt, Michael Riegler, Pal Halvorsen, "A multi class image dataset computer aided for gastrointestinal disease detection", MMSys '17, June 20–23, 2017, Taipei, Taiwan.
[4] Amit Kumar Kundu, Shaikh Anowarul Fattah and Mamshad Nayeem Rizve, "An automatic bleeding frame and region detection scheme for wireless capsule endoscopy videos based on interplane intensity variation profile in normalized RGB color space", Journal of Healthcare Engineering, Feb, 2018.
[5] Ouiem Bchir, Mohamed Maher Ben Ismail and Nada Alzahrani," Multiple bleeding detection in wireless capsule endoscopy", Springer signal, image and video processing, July, 2018.
[6] Mohsen Hajabdollahi, Reza Esfandiarpoor, S.M.Reza Soroushmehr,Nader Karimi, Shdrokh Samavi, Kayvan Najarian, " Segmentation of bleeding regions in wireless capsule endoscopy images; an approach for inside capsule video summarization", computer vision and pattern recognition , Feb, 2018.
[7] Meryem Souaidi, Abdelkaher Ait Abdelouahad, Mohamed EI Ansari, "A fully automated ulcer detection system for wireless capsule endoscopy images", IEEE, May, 2017.
[8] T.Dassopoulos, A.Karargyris, S.Makrogiannis and N.Bourbakis, " A preliminary study for automatic accurate detection of adenomatous polyps in the small intestine", IEEE,2017.
[9] Jia et al, "Accurate and efficient polyp detection in wireless capsule endoscopy images", United States patent, Aug, 2017.
[10] Mohamed EI Ansari and Said Charfi, "Computer aided system for polyp detection in wireless capsule endoscopy images", IEEE, 2017.
[11] Mustain Billah and Sajjad Waheed, "Gastrointestinal polyp detection in endoscopic images using an improved feature extraction method", Springer Biomed Eng lett, Sep, 2017.
[12] Yixuan yuan, Xiwen Yao, Junwei Han, Lei Guo and Max Q.-H. Meng, "Discriminative joint feature topic model with dual constraints for WCE classification", IEEE transactions on cybernetics, 2017.
[13] Yixuan Yuan, Baopu Li and Max Q.-H. Meng," WCE abnormality detection based on saliency and adaptive locality constrained linear coding", IEEE transactions on automation science and engineering, 2016.
[14] Herbert Bay, Andreas Ess, Tinne Tuytelaars, Luc van Gool," Speeded-Up Robust Features", Computer vision & image understanding 110 (2008), 346-359.
[15] Shreyas N Raj, Vijayalakshmi Niar, "Comparison study of algorithms used for feature extraction in facial recognition",International Journal of Computer Science & Information Technology, Vol 8(2),2017,163-166.
[16]. K.Nirmala and Dr. A.Subramani, " Content Based Image Retrieval System Using Auto Color Correlogram", Journal of Computer Applications (JCA) ISSN: 0974-1925, Volume VI, Issue 4, 2013.
[17] Nidhi Singhai, K. Shandilya "A Survey On: Content Based Image Retrieval Systems", International Journal of Computer Applications vol 4, no.2, pp.975 – 8887 , July 2010.
[18] C.H. Lin, R.T. Chen and Y.K. Chan, "A smart content-based image retrieval system based on color and texture feature", Image and Vision 12. Computing vol.27, pp.658–665, 2009.
[19] Dr. K. Seetharaman, S. Sathiamoorthy, "An improved edge direction histogram and edge orientation auto correlogram for an efficient color image retrieval", ICACCS, pp. 19-21, 2013.
[20] Shereena V. B, Julie M.David, "Significance of dimensionality reduction in image processing", Signal & Image Processing an International Journal, vol6, no3, June 2015.
[21] Dawood Al Chanti, Alice Caplier," Improving bag of visual words towards effective facial expressive image classification, Intitute of Engineering Univ Grenoble Alpes, Jan 2018.
[22] Youguo Li, Haiyan W G, "A clustering method based on K-means algorithm", Physics Procedia 25(2012), 1104-1109.
[23] B.R.Suralkar, A.H.Karode, Priti W. Pawade,"Texture image classification using Support Vector Machine", International Journal of Computer Technology Application, vol 3(1), 71-75, 2012.
[24] www.mathworks.com and www.wikipedia.com.
[25]R. Visalakshi, R. Ponnusamy, K. Manikandan, "Literature Survey of Data Mining Clustering Algorithms", South Asian Journal of Research in Engineering Science and Technology, vol.1, pp.310-313, 2016.


ISSN: 2233-7857 IJFGCN

[26]R. Ponnusamy, S. Sathiamoorthy, R. Manikandan, "A Review of Image Classification Approaches and Techniques", International Journal of Recent Trends in Engineering and Research", pp 1-5, 2017.
[27]. Kennedy VJ, Eberhart RC. Particle swarm optimization. Proceedings of the IEEE International Joint Conference on Neural Networks; December 1995; Perth, Wash, USA: pp. 1942–1948.
[28]. Kennedy J, Eberhart RC, Shi Y. *Swarm Intelligence*. Morgan Kaufmann; 2002.
[29]. Shi Y, Eberhart RC. A modified particle swarm optimizer. Proceedings of the IEEE Congress on Evolutionary Computation; May 1998; Anchorage, Alaska, USA: pp. 69–73.
[30]. Ardjani F, Sadouni K. Optimization of SVM multiclass by particle swarm (PSO-SVM) *International Journal of Modern Education and Computer Science*. 2010;2(2):32–38.
[31]R. Ponnusamy, S. Sathiamoorthy, "An Efficient Gastrointestinal Hemorrhage Detection and Diagnosis Model for Wireless Capsule Endoscopy", International Journal of Recent Technology and Engineering, 2020.
[32]. Ren Y, Bai G. Determination of optimal SVM parameters by using GA/PSO. *Journal of Computers*. 2010;5(8):1160–1168.
[33] Hussam Ali, Mussarat Yasmin, Muhammad Sharif, Mubashir Husain Rehmani, "Computer assisted gastric abnormalities detection using hybrid texture descriptors for chromoendoscopy images", Computer methods & programs in biomedicine 157(2018) 39-47.


ISSN: 2233-7857 IJFGCN